CHAPTER 15

Methods Used to Determine the Fracture Toughness of Aggregate Filled Reinforced Polymer Composites

Huseyin ARIKAN
Necmettin Erbakan University, Türkiye

Ekrem OZTURK
Necmettin Erbakan University, Türkiye

To Cite This Chapter:
Arikan, H. & Ozturk, E. (2023). Methods Used to Determine the Fracture Toughness of Aggregate Filled Reinforced Polymer Composites. In H. Arikan, Y. Uzun & I. Cetin (Eds.), *Current Studies in Basic Sciences, Engineering and Technology 2023* (pp. 145–158). ISRES Publishing.

Introduction

Reinforced polymer composites are materials formed by combining mineral aggregates and reinforcing materials with polyester resin. These materials are ideal for a variety of construction, rehabilitation, and repair applications due to their fast hardening and high-strength properties.

Polymer composites (PCs) are brittle materials, and their fracture behavior is affected by several factors such as the composition of the material, the type and geometry of the reinforcing material, the resin system, and environmental conditions. Different methods are used to characterize the fracture behavior of PCs. These methods aim to determine the stress intensity factor (K). K is an important parameter used to determine the rate of propagation of the crack and the fracture strength of the material.

In this chapter, the main methods used to characterize the fracture behavior of PCs will be discussed. The methods will be classified as the initial notch depth method, the compliance method, the J-integral method, and the critical opening (CMOD) method. The theoretical foundations of the methods and the advantages and disadvantages of their practical applications will be examined.

Reinforced polymer composite (PC) is formed by combining mineral aggregates and reinforcing materials with polyester resin. PCs with resin system; Due to its fast hardening and high strength properties, it is used in a variety of construction, rehabilitation, and repair applications such as bridges, pipelines, and other types of construction ((Hassani Niaki, 2023; Vipulanandan & Dharmarajan, 1987; Guerrini, 2000; Barnaby & Dikeou, 1984; Fowler, 1983).

At the same time, many studies have been carried out to characterize the fracture behavior in systems where cement is used as aggregate. (Avcı & et. al,2004,2005; Arikan & et. Al,2004; Samanci, 2012; Dharmarajan & Vipulanandan, 1988; Vipulanandan &

Dharmarajan, 1989).

Although PCs are brittle materials, the assumptions in the mechanics of direct elastic fracture and the mechanics of elastic-plastic fracture do not always give the correct result. Therefore; Characterizing the refractive behavior; to determine the stress intensity factor; Different methods such as the initial notch depth method, compliance method, J-integral method, and critical opening (CMOD) were used (Avcı & et. al,2004,2005; Arikan & et. Al,2004; Samanci, 2012; Dharmarajan & Vipulanandan, 1988; Vipulanandan & Dharmarajan, 1989).

1. Aggregate Filled Reinforced Polymer Composites

It is a type of composite material in which there are grains over millimeters in size in a matrix. For example, polymer concrete, which is a type of polymer composite, or cement-based concrete can be given.

As described above, the material obtained by holding various grains together by bonding them with a binder is called particle additive composite in general classification. If a thermosetting matrix is used as a binder, it is called a polymer composite. If the grains that form polymer composites are sand and resin is used as a binder, such polymer composites are also called polymer concrete. The polymer composite expression used in this study refers to polymer concrete.

Polymer composites have a single property depending on the formulation. These;

- Fast hardening at ambient temperature
- High tensile, flexural, and compressive strength
- Good adhesion to most surfaces
- A low permeability to corrosive properties or water, a good chemical resistance

Polymer composite components are briefly explained below.

- Hardeners for monomers: Hardener types for monomers are benzoyl peroxide (BPO), lauryl, and methyl ethyl ketone peroxide (MEK).
- Accelerators for monomers: These exist in the form of terthierdimethylaniline. They are slightly strawberry-colored liquids. They disperse quickly in monomers.

Sands: All sands used in connection with monomer systems should consist mainly of silicon, quartz, granite, limestone, and other high-quality materials. Sands should generally be dried. They must be cleaned of dirt, asphalt, and other organic materials. Moisture on sands reduces the bonding strength of most monomer systems and epoxy resins. Unless otherwise stated, sands should not have surface moisture. In some systems, the humidity content can be up to 3%. In certain cases, the humidity should be less than 1% (David, 1986).

Properties, Types and Uses of Polymer Composites

Polymer composites are preferred because they have higher strength compared to traditional concrete composites in applications where resistance to water and chemicals is required and they need to be lightweight. This material has a wide range of uses, for example, it has found a wide range of uses in building construction, stairs, pipelines, insulators, electrical and communication lines, cable lines, etc.

Polymer composite was first used in the construction of bench bodies. Later, it is produced from this material in applications such as high-speed milling and precision drilling machines.

Polymer composite is an artificial material with a high filling agent. While normal concrete composites are created with binder materials such as sand, water, and cement, polymer composites contain materials such as synthetic resin as a binding material, silicate-type materials as an additional material, and calcium carbonate as a filling material. The properties of polymer composites depend on the type and properties of the binder used, as well as the properties of the aggregates. The reason why aggregates such as sand are preferred is that they have less plastic deformation than other materials. Polyester resin, methacrylic resin, and epoxy resin are preferred as binding materials used in polymer composites. In practice, polymer composites with epoxy resins are used for mass production in applications such as bench bodies.

The strength of the polymer composite decreases significantly as the moisture content of the additional materials increases. The particles of these materials are dried by fire. When the plastic shaping process continues for a long time, the particle size increases. Polymer composite with small particles requires the use of more resin, which negatively affects the strength properties and hardness resistance of the polymer composite.

In addition to mechanical and thermal properties, plastic deformation and rest are important. In the experiments, it was observed that epoxy resin polymer composites had a higher shape change, while acrylic resin composites had less shape change. At the same time, epoxy resins show ductility at temperatures up to 50 °C. For the additional material to be thoroughly mixed, the synthetic resin must have a low viscosity. Table 1 gives the physical properties of polymer composite materials.

High-speed machine bodies made of polymer composites can operate at a higher frequency than bench bodies made of other materials. A particular advantage of polymer composite machine tools is the absence of critical resonances within the bench work area (Schulz 1984).

In the methacrylic resin composite formed with iron, an increase in friction strength was obtained compared to the construction from pure polymer composite, and an increase in absorption and rigidity compared to iron construction. The 3420 kg grinding machine uses 2100 kg of polymer composites, resulting in six times higher absorption and higher rigidity on the slide paths. The vibration of the polymer composite was reduced by 10 μm before filling and by 1 μm after filling. At the same time, natural frequencies increased from 115 Hz to 195 Hz and from 150 Hz to 232 Hz (Acherkan, 1973).

Tablo 1.
Physical Properties of Aggregate Filled Reinforced Polymer Composites

Physical Properties of the Material	Epoxy Composite	Polyester Composite
Density (kg/dm3)	2.02	1.98
Flexural Elasticity Modulus (GPa)	4-7	2.5-4.5
Flexural Strength (MPa)	12-25	5-15

2. Fracture Mechanics

Fracture mechanics and fracture toughness test methods constitute one of the main topics in the field of materials engineering, which is critical for studying the durability of materials, the propagation of cracks, and fracture behavior.

The most important aspect of fracture mechanics is that it examines fracture problems by considering the factors that increase crack and stress concentration in materials under stress. Mechanical cracks can occur during the production of materials used in machinery and construction. During the manufacture of materials, hairline cracks can be found for various reasons. Stress concentration occurs around these cracks and causes fracture. Cracks caused by stress concentration can also be at stresses lower than the yield stress of the material used. Materials whose structure contains capillary cracks and large cavities that undergo plastic deformation usually show brittle fracture (Kayalı & et al., 1983).

Theories and experiments have been developed that study the primarily brittle fracture character of metallic materials. These experiments are not sufficient for a construction engineer or researchers who are closely interested in fracture. With fracture mechanics analysis, both the cause of damage to the material can be understood and the formation of any cracks during manufacturing and use can be prevented.

In fracture mechanics, the parameters related to fracture are fracture toughness or stress strength factor (GCF). The stress intensity factor is expressed by the symbol "K". Stress intensity factor K is a parameter that determines the stress area around the crack, which depends on the geometric shape of the material, the loading shape, and the location and orientation of the crack.

The fracture toughness of a material can be defined as its capacity to carry loads when there are cracks in the material or its ability to deform plastically. Material toughness can be expressed by the critical stress intensity factor under plane stress conditions (KC) and plane deformation conditions (KIC). These behaviors are valid within the framework of Linear Elastic Fracture Mechanics (LEKM).

2.1 Linear Elastic Fracture Mechanics

To perform stress analysis of cracks in elastic objects, it is necessary to know the bound motion of the crack surface. Crack propagation behavior is seen in three types. This can include one, two, or all three of these three types.

Type I is the most common and more critical opening mode than the others. The two fracture surfaces are opened in opposite directions to each other and perpendicular to each other. In type II slip mode, the crack surfaces move in the opposite direction on the x-z plane. In Type III rupture mode, the crack proceeds inversely symmetrically concerning the x-y and x-z planes. The two fracture surfaces slide in a parallel direction with a line in front of the crack relative to each other. Stress deformations in isotropic materials near the crack tip were found by Irwin (Irwin, 1957). The intensity factors of crack tip strain are as follows for each mode. Here, K_I, K_{II}, and K_{III} are stress intensity factors for mode I, mode II, and mode III, respectively. The Mode I crack tip stress zone distribution and coordinate system representation are as shown in Figure 1.

Figure 1.

Mode I Crack Tip Stress Zone Distribution and Coordinate System

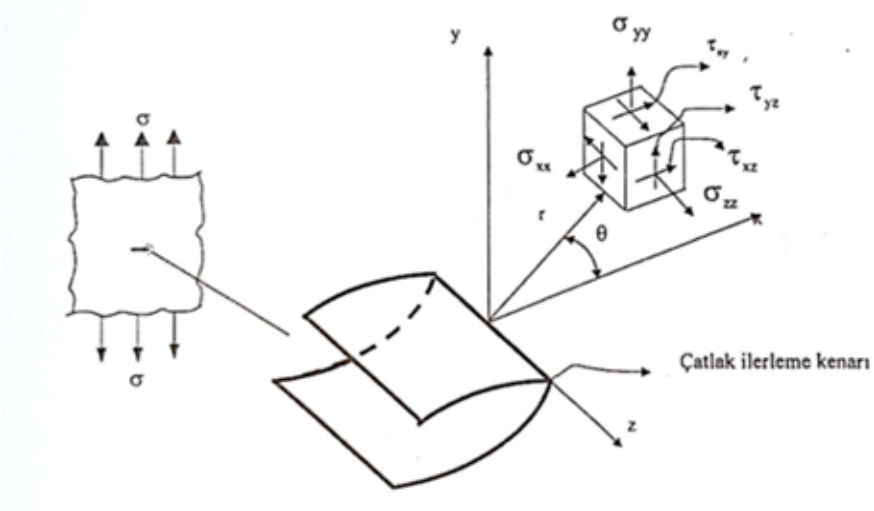

The stresses at the crack end are as follows;

$$\sigma_{xx} = \frac{K_I}{(2\pi r)^{1/2}} \mathbf{Cos}\frac{\theta}{2}\left(1 - \mathbf{Sin}\frac{\theta}{2}\mathbf{Sin}\frac{3\theta}{2}\right)$$

$$\sigma_{yy} = \frac{K_I}{(2\pi r)^{1/2}} \mathbf{Cos}\frac{\theta}{2}\left(1 + \mathbf{Sin}\frac{\theta}{2}\mathbf{Sin}\frac{3\theta}{2}\right)$$

$$\tau_{zz} = \frac{K_I}{(2\pi r)^{1/2}} \mathbf{Cos}\frac{\theta}{2}\left(\mathbf{Cos}\frac{\theta}{2}\mathbf{Cos}\frac{3\theta}{2}\mathbf{Sin}\frac{\theta}{2}\right)$$

$$\sigma_{zz} = \frac{K_I}{(2\pi r)}\left(2v\mathbf{Cos}\frac{\theta}{2}\right)$$

$$\tau_{yz} = \tau_{zx} = 0$$

As in Figure 2, the shape changes of the opened crack at the point at the distance r are as follows. where ν: is Poisson's ratio, σ_{XX} : is the stress value on the x-axis, σ_{YY} : is the stress value on the y-axis, and σ_{ZZ} : is the stress value on the z-axis. K_I: is the stress intensity factor for mode I, E: is the modulus of elasticity, θ: is the angle r makes with the x-axis. U, V, W are the displacements on the x, y, z axes, respectively.

$$u = \frac{K_I}{E}\left(\frac{r}{2\pi}\right)^{1/2}(1+v)\left[(2k-1)\mathbf{Cos}\frac{\theta}{2} - \mathbf{Cos}\frac{3\theta}{2}\right]$$

$$v = \frac{K_I}{E}\left(\frac{r}{2\pi}\right)^{1/2}(1+v)\left[(2k+1)\mathbf{Sin}\frac{\theta}{2} - \mathbf{Sin}\frac{3\theta}{2}\right]$$

$$\acute{y}w = -v^{\cdot}\frac{K_I}{E} \quad (\textit{Düzlem gerilme hali için } 0'd \;\;)$$

$$v^{\cdot} = v,\; k = \frac{(3-v)}{(1+v)} \quad (\textit{Düzlem gerilme hali için })$$

$$v = 0,\; k = 3 - 4v \quad (\textit{Düzlem deformasyon hali için})$$

Stresses for the Mode II state;

$$\sigma_{xx} = \frac{K_{II}}{(2\pi r)^{1/2}} \mathbf{Sin}\frac{\theta}{2}(2 + \mathbf{Cos}\frac{\theta}{2}\mathbf{Cos}\frac{3\theta}{2})$$

$$\sigma_{yy} = \frac{K_{II}}{(2\pi r)^{1/2}} \mathbf{Sin}\frac{\theta}{2}\mathbf{Cos}\frac{\theta}{2}\mathbf{Cos}\frac{3\theta}{2})$$

$$\tau_{xy} = \frac{K_{II}}{(2\pi r)^{1/2}} \mathbf{Cos}\frac{\theta}{2}(1 - \mathbf{Sin}\frac{\theta}{2}\mathbf{Sin}\frac{3\theta}{2})$$

$$\sigma_{zz} = v(\sigma_{xx} + \sigma_{yy})$$

$$\tau_{yz} = \tau_{zx} = 0$$

The displacements equation is found as follows;

$$U_x = \frac{K_{II}}{E}(\frac{r}{2\pi})^{1/2} \mathbf{Sin}\frac{\theta}{2}\left[(2 - 2v\mathbf{Cos}^2\frac{\theta}{2}\right]$$

$$U_y = \frac{K_{II}}{E}(\frac{r}{2\pi})^{1/2} \mathbf{Cos}\frac{\theta}{2}\left[(-1 + 2v\mathbf{Sin}^2\frac{\theta}{2}\right]$$

$$w = 0$$

Stresses and displacements for Mode III state;

$$\tau_{xz} = \frac{K_{III}}{(2\pi r)^{1/2}} \mathbf{Sin}\frac{\theta}{2}$$

$$\tau_{yz} = \frac{K_{III}}{(2\pi r)^{1/2}} \mathbf{Cos}\frac{\theta}{2}$$

$$\sigma_{xx} = \sigma_{yy} = \sigma_{zz} = \tau_{xy} = 0$$

$$u = v = 0$$

$$w = \frac{K_{III}}{E}\left[\frac{2r}{\pi}\right]^{1/2} \mathbf{Sin}\frac{\theta}{2}$$

2.2. Elastic-Plastic Fracture Mechanics

In many materials, it is almost impossible to explain fracture behavior by linear elastic fracture mechanics and an alternative fracture model is required. Elastic-plastic fracture mechanics are applied for materials that exhibit nonlinear behavior (such as plastic deformation). One of the parameters that characterize elastic-plastic behavior is the crack tip displacement (CTOD) and the other is J-integral. The critical value of CTOD and J-integral establishes size-independent fracture toughness and gives a large amount of crack tip plastic behavior (Anderson,1991).

2.2.1. Crack Tip Opening Displacement (CTOD) Method

When Wells tried to determine the fracture toughness value in a steel structure, he found that these materials were too tough to be characterized by linear elastic fracture mechanics. Although high toughness is desirable, the theory of fracture mechanics could

not be applied to such an important material. Wells, while examining the crack surface; He noticed that the crack was sharp at first, then it was closed by plastic deformation and the closure in the crack increased in proportion to the fracture toughness. This observation has led to the suggestion of the use of crack tip opening as a measure of fracture toughness. Today, this parameter is known as "crack tip displacement (CTOD)" and is used as a parameter of fracture (Anderson,1991).

A single edge notch bending (SENB) specimen is preferred to determine the CTOD value. As shown in Figure 2, the CTOD value is found by determining the amount of crack opening (CMOD) V_P. V_P is the amount of crack opening (CMOD). The amount of crack tip opening is expressed in δ. Figure 3 shows the measurement of V_P with clip-gage.

the connection between δ and clip-gage displacement;

$$\delta = \delta_{el} + \delta_{pl}$$

$$\delta = \frac{K^2(1-v^2)}{2\sigma_y E} + \frac{0.4(W-a)V_p}{0.4W + 0.6a + z}$$

It is found with expressions (ASTM E-1290 1993).

Here;

- K is the fracture toughness value found by the initial notch depth method.
- v is the Poisson ratio.
- W is the material width.
- A is the initial notch depth.
- V_P is the amount of crack opening (CMOD).

Basically, by measuring the critical value of the CTOD, the maximum allowable crack length for the plane stress state can be found. In the case of plane shape change, although some finite element solutions can be used, a complete analytical solution cannot be made.

Figure 2.
Representation of δ in a Single Edge Notched Bending (SENB) Specimen

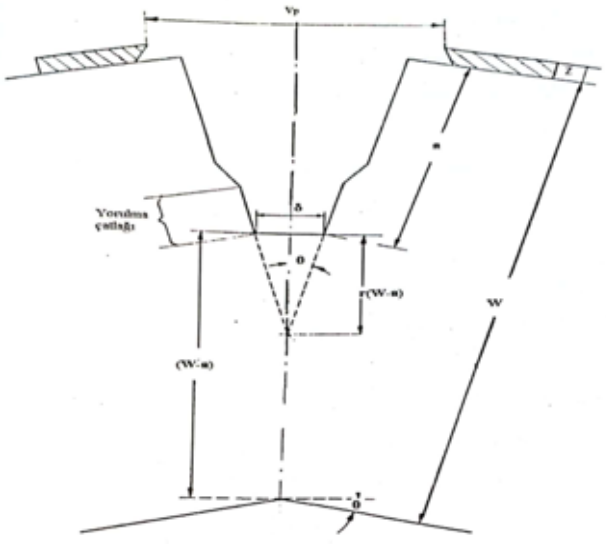

Figure 3.
Measurement of V_P Value with Clip-Gage

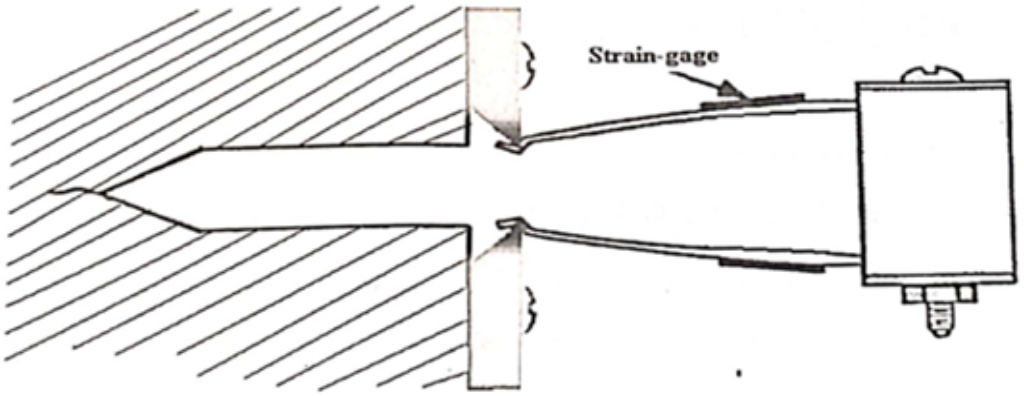

2.3. Fracture Toughness Test Methods

A fracture toughness test measures a material's resistance to crack growth. This test can determine both a single fracture toughness value and the resistance curve. These values are toughness parameters such as fracture toughness (K), J-integral (J), or crack tip opening displacement (CTOD) plotted against crack growth. A single toughness value is usually sufficient to describe a test that has undergone cleavage fracture. This fracture mechanism is typically unstable.

The ASTM E399 standard prescribes four sample formats. These are compact, single-edge notched bending (SENB), arc-shaped, and disc-shaped specimens. In bending specimens with a single edge notch, thickness is usually shown as B, width W. In samples with pre-cracks, the crack depth is expressed as a and the ratio of the crack to the sample width is expressed as a/W. Thus, a, B, and *a*/*W* values are considered in the sample design.

In most mechanical tests (fracture toughness and others); The healthy conduct of the experiment affects the experimenter as much as the procedure in the test standard, and invalid results can often be obtained due to these errors. If the plastic region at fracture is too large, it is impossible to obtain the valid K_{IC} value.

ASTM E-399 recommends an accurate approach to determining sample sizes due to very careful measurement requirements. Specimen sizes for K_{IC} testing are valid if they meet the following requirements.

$$B,(W-a) \geq 2,5\left[\frac{K_{IC}}{\sigma_{ys}}\right]^2$$

Here, to calculate the required sample sizes, the user must use the estimated K_{IC} value. While making this estimation, it can benefit from the K_{IC} values of similar samples.

According to ASTM E-399, the maximum value of the tensile intensity factor K_{max} in one cycle during the fatigue pre-crack should not be greater than 0.8 K_{IC}. When reaching the final size of the crack, the K_{max} should not be less than 0.6 K_{IC}. The fatigue value should always be less than the K_{IC}.

Load and displacement are observed when loading is performed to advance the

crack on a pre-cracked test specimen. There are three types of load-displacement curves, as shown in Figure 4. Critical load P_Q is defined in several ways, depending on the type of curve.

- In Type I, a 5% secant curve must be drawn to obtain the P_5 charge. The critical load here is

  $P_Q = P_5$.
- In type II, there is unstable fissure progression. The critical load here is as shown in the figure.
- In Type III, the critical load is the same as the maximum load.

The crack length should be measured from the crack surface. First, the critical load and crack length are calculated, and the fracture toughness K_Q is calculated from the following relation.

Figure 4. *Typical Load-Displacement Graph*

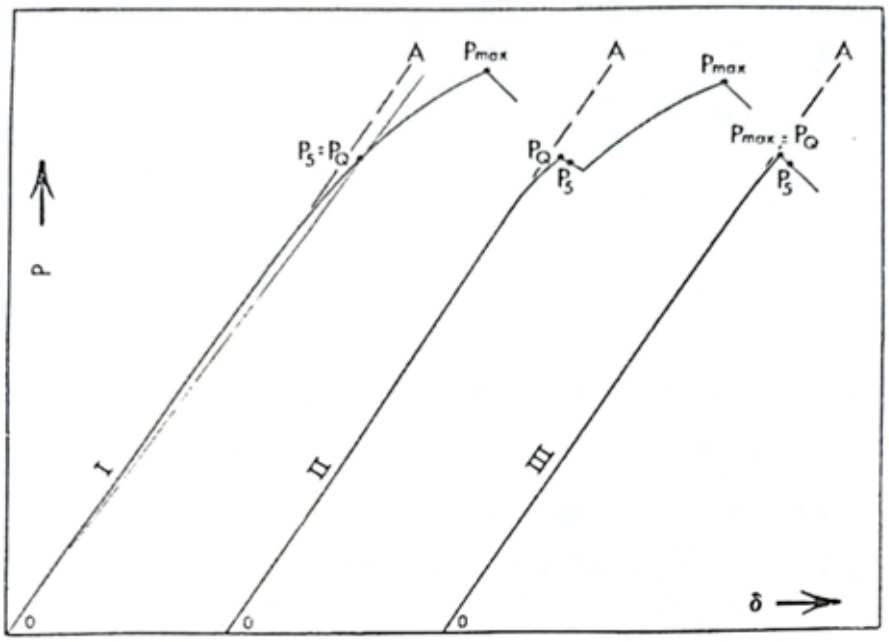

$$K_Q = \frac{P_Q}{B\sqrt{W}} f\left(\frac{a}{b}\right)$$

where $f(a/W)$ is a dimensional function of the notch ratio. It is given in the ASTM standard for the three-point bending test and S/W = 4 as follows. Here, S is the inter-support spacing, and W is the material width (Vipulanandan, & Dharmarajan, 1988).

$$f\left(\frac{a}{W}\right) = 1.93 - 3.07\left(\frac{a}{W}\right) + 14.53\left(\frac{a}{W}\right)^2 - 25.11\left(\frac{a}{W}\right)^3 + 25.80\left(\frac{a}{W}\right)^4$$

For other sample types, $f(a/W)$ values are also available in ASTM standards. Figure 5

shows a picture of a notched glass fiber-reinforced polymer composite specimen that has undergone a three-point bending test to determine fracture toughness.

Figure 5. *Notched Aggregate Filled Reinforced Polymer Composite Specimen (After Three-Point Bending Test)*



2.3.1. Initial Notch Depth Method

In linear elastic fracture mechanics, the amount of crack propagation cannot be clearly observed since the material is very brittle. For this reason, this method is used to determine the critical stress intensity factor of such a material and to examine the fracture behavior at different crack depths. According to the ASTM E-399 recommendation, the critical load for a valid K value is selected according to which of the charge-displacement curves given in Figure 4 is appropriate.

The graphs obtained in this study are generally like Type I. For this reason, P_5 should be taken as the critical load here, but since the K_{IC} value will be slightly higher if the maximum load is taken, the P_{max} value can be used (Brown, & Srawley, 1966). The stress intensity factor K_I concerning Mode I is expressed as follows.

$$K_I = \sigma\sqrt{a}\, f\left(\frac{a}{W}\right)$$

where σ is the net stress, a is the initial crack depth, $f(a/W)$ is the geometry factor and is given above. σ is expressed as follows for the three-point bending test.

$$\sigma = \frac{3PS}{2BW^2}$$

Here, P is the critical load, S is the distance between the bearings (for the three-point bending test), B is the material thickness, and W is the material width. The K_{IC} value is independent of the fracture thickness and the a/W value.

2.3.2. Compliyans Method

In materials with brittle fracture, the compliance technique can be used to evaluate the actual crack length and is an accurate method (13). Compliance (C) is the inverse of the slopes of a material's load-displacement or load-crack opening amount (CMOD) curves.

With this method, the complicity must be found first when finding the K_{IC} value. The compliance is found in the figure below using the load-CMOD graph (Duggan & et al., 1979).

$$C = \frac{d(CMOD)}{dP}$$

A crack size graph is created with the compliance values found from this formula. Using the slope of this graph, the KIC value is calculated from the following formula.

$$K_{IC} = \frac{PE}{2B(1-v^2)} \frac{dC}{d(a/W)}$$

2.3.3. J-integral Method

Fracture toughness is very difficult to measure due to the formation of large plastic regions at the crack tip. To overcome this problem, the J-integral method was developed (Aksoy,1984).

In an ideal brittle material with a 2a long crack inside, the amount of energy discharged if the crack grows in the face of strain;

$$G_{IC} = \frac{1}{C} \frac{d(-W + U_{el})}{d(2a)}$$

Here B is the material thickness, W is the elastic energy generated in the object due to the effect of the force P made by the force P forcing the object. The energy state within the J-integral curve developed by Rice (1968);

$$J = \int (Wdy - T)(\partial u / \partial x) dx$$

Here, T stands for the refraction vector. This equation holds true in both cases, whether linear elastic or elastic-plastic behavior.

If the material exhibits linear elastic behavior, the J-integral energy becomes equal to the amount of discharge.

In elastic-plastic behavior, the J-integral is expressed as follows;

$$G_{IC} = \frac{1}{B} \frac{dU}{d(2a)}$$

Here, U is the energy exchange. When the J-integral reaches a certain critical value (J_C and J_{IC}), unstable crack growth begins.

There are three methods for experimental determination of the J-integral.

- Different initial crack bottom sample technique (Bucci, 1971).
- Deep-fissured specimen technique (Begley, 1971).
- Cracked vs. non-cracked sample technique (Rice, 1973).

Mindess et al (1987) calculated the critical J-integral of the sample at maximum load using the third method, thinking that it works well in polymer composites.

When the crack begins to progress, there is potential change. Figure 6 shows the load-displacement graph of the notched and non-notched material. The following method is followed in the determination of the J-integral (Ziegeldorf,1983); The area (A_t) under the charge-displacement curve (P-δ) of the notched material is subtracted from the area (A_u) under the P-δ graph of the unnotched material charged with the same

load. The value obtained from here is put into the formula below to find the critical J-integral (J_{IC}) value.

$$J_{IC} = \frac{2(A_t - A_u)}{d(b-a)}$$

Here, b is the width of the specimen.

The J_{IC} obtained from this is substituted below and the K_{IC} value is calculated (Vipulanandan, C., & Dharmarajan,1987).

$$K_{IC}^2 = \frac{EJ_{IC}}{1-v^2}$$

Figure 6. *Load-Displacement Graph of Notched and Non-notched Material*

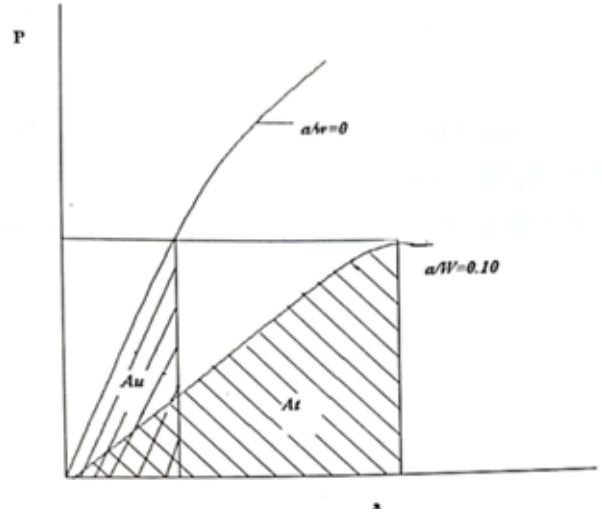

References

Hassani Niaki, M. (2023). "Fracture mechanics of polymer concretes: A review." *Theoretical and Applied Fracture Mechanics, 125.*

Vipulanandan, C., & Dharmarajan, N. (1987). "Flexural behavior of polyester polymer concrete." *Cement and Concrete Research, 17,* 219–230.

Guerrini, G. L. (2000). "Applications of high-performance fiber-reinforced cement-based composites." *Applied Composites Materials, 7,* 195–207.

Barnaby, D., & Dikeou, J. T. (1984). "Applications of permanent precast polymer concrete forms for concrete rehabilitation." *Transportation Research Record No: 1003, Transportation Research Board,* 46–49.

Fowler, D. W. (1983). "Polymers in Concrete." *Handbook of Structural Concrete, McGraw-Hill Book.*

Avci, A., Arikan, H., & Akdemir, A. (2004). "The fracture behavior of glass fiber

reinforced polymer composite." *Cement and Concrete Research, 34,* 429–434.

Avci, A., Akdemir, A., & Arikan, H. (2005). "Mixed-mode fracture behavior of glass fiber reinforced polymer concrete." *Cement and Concrete Research, 35,* 243–247.

Arikan, H., Avci, A., & Akdemir, A. (2004). "Fracture behavior of steel fiber reinforced polymer composite." *Polymer Testing, 23,* 615–619.

Samanci, A. (2012). "Fracture behavior of woven steel fiber reinforced, and sand particle filled polymer composites." *Construction and Building Materials, 26(1),* 167–171.

Dharmarajan, N., & Vipulanandan, C. (1988). "Effect of temperature on the fracture properties of epoxy-polymer concrete." *Cement and Concrete Research, 18(2),* 265–276.

Dharmarajan, N., & Vipulanandan, C. (1988). "Critical stress intensity factors of epoxy mortar." *Polymer Engineering and Science, 28(18),* 1182–1191.

Vipulanandan, C., & Dharmarajan, N. (1989). "Fracture properties of particle-filled polymer composites." *Journal of Composite Materials, 23,* 846–860.

David, W. F. (1986). "Guide for The Use of Polymers in Concrete." *ACI Journal Committee Report, 548.IR,* 789-829.

Schulz, H. (1984). "Statical and Dynamical Behavior of Mechanics Tool Frames Made of Polymer Concrete." *Fourth International Congress, Darmstadt, Sept,* 19–21.

Acherkan, N. (1973). *Machine Tool Design.* Mir Publisher, Moskova.

Kayalı, E. S., Ensari, C., & Diken, F. (1983). *Metalik Malzemelerin Mekanik Deneyleri.* ITU Matbaası, Istanbul, 91-94.

Irwin, G. R. (1957). "Analysis of Stress and Strain Near the End of Crack Traversing a Plate." *Transaction ASME, Journal of Applied Mechanics, 24.*

Anderson, T. L. (1991). *Fracture Mechanics: Fundamentals and Applications.* CRC Press, Boston.

Brown, W. F., & Srawley, J. E. (1966). *ASTM, STP 410, PA.*

Duggan, T. V., Proctor, M. W., & Spence, L. J. (1979). "Stress intensity calibrations and compliance functions for fracture toughness and crack propagation test specimens." *International Journal of Fatigue, 1(1),* 37-47.

Aksoy, T. (1984). *Kırılma Mekaniği.* Dokuz Eylül Üniversitesi, Izmir, 20-24.

Rice, J. R. (1968). "A Path Independent Integral and the Approximate Analysis of Strain Concentration by Notches and Cracks." *pp. 375-386.*

Bucci, R. C., Paris, P. C., Landes, J. D., & Rice, J. R. (1971). *ASTM, STP 514, PA.*

Begley, J. A., & Landes, J. D. (1971). *ASTM, STP 514, PA.*

Rice, J. R., Paris, P. C., & Merkle, J. G. (1973). *ASTM, STP536, PA.*

Mindess, S., Banthia, N., & Yan, C. (1987). "The Fracture Toughness of Concrete Under Impact Loading." *Cement and Concrete Research, 17,* 231-241.

Ziegeldorf, Z. (1983). *Fracture Mechanics of Concrete.* Elsevier Science Publishers, 371-409.

About The Authors

Huseyin ARIKAN is a Professor of Mechanical Engineering at Necmettin Erbakan University in Konya, Turkey. He holds a Professor in Mechanical Engineering from Necmettin Erbakan University. His main areas of interest are Composite Materials, Fracture Mechanics, and Materials Desing and Manufacturing.
E-mail: harikan@erbakan.edu.tr, **ORCID:** 0000-0003-1266-4982

Ekrem OZTURK received a third bachelor's degree from the Department of Mechanical Engineering at Selcuk University in 2013. He completed her master's degree at Selcuk University in 2015 and received PhD degree at Necmettin Erbakan University in 2021. He is a Research Assistant in the Department of Mechanical Engineering at Necmettin Erbakan University in Konya, Turkey. His research areas are manufacturing, material design and behavior, mechanics of materials, sheet metal forming, hydroforming, joining technologies, and finite element analysis.
E-mail: eozturk@erbakan.edu.tr, **ORCID**: 0000-0002-0446-4211

Similarity Index :
The similarity index obtained from the Ithenticate software for this book chapter is 15%.